Rapid 3D rockfall susceptibility assessment of the Orašac rock slope, Croatia

Hrvoje Lukačić[(1)], Josip Katić[(1)], Sanja Bernat Gazibara[(1)], Snježana Mihalić Arbanas[(1)], Martin Krkač[(1)*]

1) University of Zagreb, Faculty of Mining, Geology and Petroleum Engineering, Pierottijeva 6, 10000 Zagreb, Croatia (mkrkac@rgn.hr)

Abstract This paper presents a rockfall susceptibility assessment on a detailed (cliff) scale, by using the data from the high-resolution 3D point cloud obtained by unmanned aerial vehicle (UAV) digital photogrammetry. The studied limestone rock slope is located in Dubrovnik-Neretva County, south Croatia. Discontinuity orientations, required for 3D rockfall susceptibility assessment, were manually mapped, using the structural geology toolbox Compass, integrated within CloudCompare v2.12, providing information about the number and orientation of individual discontinuity planes, the number of discontinuity sets and weighted density concentrations associated with certain discontinuity set. Based on the acquired input data, a 3D rockfall susceptibility assessment was done for planar failure, wedge failure, and flexural toppling failure. Rockfall susceptibility assessment consisted of performing spatial kinematic analysis for normal and overhanging slopes based on the Markland test and highlighting points in the 3D point cloud susceptible to certain types of failure. Based on discontinuity orientations and orientations of the points in the point cloud, the Kinematic Hazard Index was calculated for every point in the 3D point cloud, and potential rockfall source areas were highlighted. The Kinematic Hazard Index was calculated by in-house MATLAB code which enables rapid 3D rockfall susceptibility assessment considering complex slope topology in both normal and overhanging areas of the studied rock slope.

Keywords rockfall susceptibility assessment, 3D point cloud, discontinuity mapping, UAV

Introduction

Rockfall hazard and risk assessment is a crucial part of responsible spatial planning and construction in rock masses due to the sudden occurrence and unpredictable nature of rockfall events (Evans and Hungr 1993). Due to that reason, numerous research exists regarding to rockfall susceptibility, hazard and risk assessment, in both, regional (e.g Loye et al. 2009; Rossi et al. 2021) and detailed (cliff size) scales (e.g. Gigli et al. 2012; Matasci et al. 2017; Menegoni et al. 2021). In recent years, a rockfall susceptibility analysis has often been performed on the data obtained from remote sensing methods (Matasci et al. 2017, Farmakis et al. 2020, 2023). The most widely used remote sensing methods for obtaining data for susceptibility analysis on a detailed scale are terrestrial laser scanning and digital photogrammetry (Menegoni et al. 2019, Fanti et al. 2013). LiDAR (Light Detection and Ranging) is a fully automated remote sensing technology that uses light beams to acquire data about slope topology (Wehr & Lohr 1999), while digital photogrammetry uses images captured with a high-resolution camera with appropriate overlap (Luhmann et al. 2014). From both techniques, it is possible to generate high-resolution 3D point clouds of vertical rock slopes.

Based on the acquired point cloud data, engineering geological mapping can be done by applying manual and semi-automated mapping techniques for obtaining discontinuity orientation, spacing, and persistence data (Battulwar et al. 2021). Applying such methods enables the collection of large amounts of discontinuity data compared to traditional field surveys. A large amount of collected discontinuity data, predominantly orientation, in combination with precise data about slope morphology, enables research to perform spatial kinematic analysis for assessing the potential of a rock slope for the occurrence of different types of failure. By performing the spatial kinematic analysis, it is possible to overcome some of the drawbacks of conventional stereonet-based analysis, like (1) uniform slope angle, (2) assumption of tightly clustered discontinuity data, (3) even spatial distribution of discontinuity planes and (4) unbiased representation of discontinuity sets (Admassu et al. 2013).

This study aims to demonstrate how the combination of engineering geological mapping using remote sensing techniques, with the help of MATLAB (MathWorks 2023) computing, can be used for producing reliable cliff scale rockfall susceptibility maps for rapid susceptibility assessment. Discontinuity planes are mapped manually using the open-source software CloudCompare (CloudCompare 2021) on a 3D point cloud, derived from Unmanned Aerial Vehicle (UAV) digital photogrammetry. The rockfall susceptibility is assessed by applying the Kinematic Hazard Index proposed by Casagli & Pini (1993).

Study area

The investigated rock slope is located on the state road DC8 (Trsteno-Orašac) in Dubrovnik-Neretva County, south Croatia. The vertical rock slope has a total length of approximately 35 meters and a maximum height of 12.30 meters. Analysed slope, with its concave shape, generally strikes NW-SE, and it is located on the hillslope dipping towards SW. The majority of the rock slope has an angle greater than 70° with an average value of 75°. The height of the studied slope ranges from four to approximately 12 meters.

The rock slope area is located near the geological contact between Paleogene, Cretaceous and Triassic deposits. According to the Basic Geological Map of Croatia (Geological survey Sarajevo 1967) and the results of field mapping, it was determined that the rock slope is composed of Paleogene alveolinic-numulitic limestones. The limestone rock is moderately strong to strong with uniaxial compression strength around 80 MPa and grey to light grey in colour. Based on the results of the engineering geological mapping, four engineering geological zones can be distinguished based on the local average slope orientation, degrees of fracturing, and weathering conditions.

Methodology

UAV data acquisition and processing

The UAV survey was undertaken in March 2023 using DJI Phantom 4 Pro V2.0. The survey was done using a manual flight mission with an average front and side overlap of 70-80% at approximately 6 meters of horizontal camera-outcrop distance. A manual flight mission was applied for collecting data for both orthophoto images as well as 3D point cloud creation. The photogrammetric survey resulted in collecting a total of 475 images in JPEG format. Images were taken by a 20-megapixel resolution on-board camera equipped with 1 1-inch CMOS sensor. All collected images were directly georeferenced using an integrated Global Navigation Satellite System (GNSS). Details of the UAV system used for this study and survey characteristics are reported in Table 1, while generated 3D point cloud is presented in Fig. 1.

High-resolution images were processed by means of the Structure from Motion (SfM) technique using Agisoft Metashape Professional software (Agisoft 2020). The final point cloud (Fig. 1) has approximately 220 million points in the .xyz file with an average point density of 271 470 points/m². As a postprocessing step, vegetation was removed using the CANUPO plugin for CloudCompare (Brodu and Lague 2012), and only points corresponding to the rock slope were filtered. After removing vegetation, approximately 43% of points remained in the point cloud, representing only the rock slope.

Table 1 Details of the UAV system and photogrammetric survey.

UAV SYSTEM	
UAV device	DJI Phantom 4 Pro V2.0
Maximum weight	1375 g
Gimbal stabilisation	3-axis
Satellite positioning system	GPS/GNSS
ON-BOARD CAMERA PARAMETERS	
Lens	8,8 mm/24 mm, f/2,8-f/11
Sensor	CMOS, 1”
FOV	85°
Photo resolution	5472 x 3078
SURVEY DETAILS	
Flight mode	Manual
Coverage area (m^2)	3536
Frontal distance from the slope (m)	6
Number of photos	475
Photos overlap (%)	70 - 80
Frame shooting interval (s)	2

Engineering geological mapping

Engineering geological mapping was performed on homogeneous engineering geological zones on the 3D point cloud model. The investigated rock slope was divided into four homogeneous engineering geological zones based on the local average slope orientation, degrees of fracturing, and weathering conditions. For each zone, structural analysis was performed. High-resolution 3D point cloud data was used to manually measure individual discontinuity orientations using the Compass tool (Thiele et al. 2017), a plugin implemented into CloudCompare v2.12 software.

When collecting discontinuity orientation data, it is necessary to detect individual discontinuity surfaces and, by using the function Plane tool, select the radius within which all points are used to calculate the orientation of the best-fit plane using the least-squares method. The number of performed measurements depended on the fracturing conditions in each engineering geological zone, varying from 24 up to 174 measurements per zone. Measured discontinuity planes were grouped into individual discontinuity sets using the Fuzzy Cluster methodology implemented into Dips 7.0 software by RocScience (RocScience 2022). Mean discontinuity set orientations were compared with the data from the field mapping to check the quality of remote sensing data.

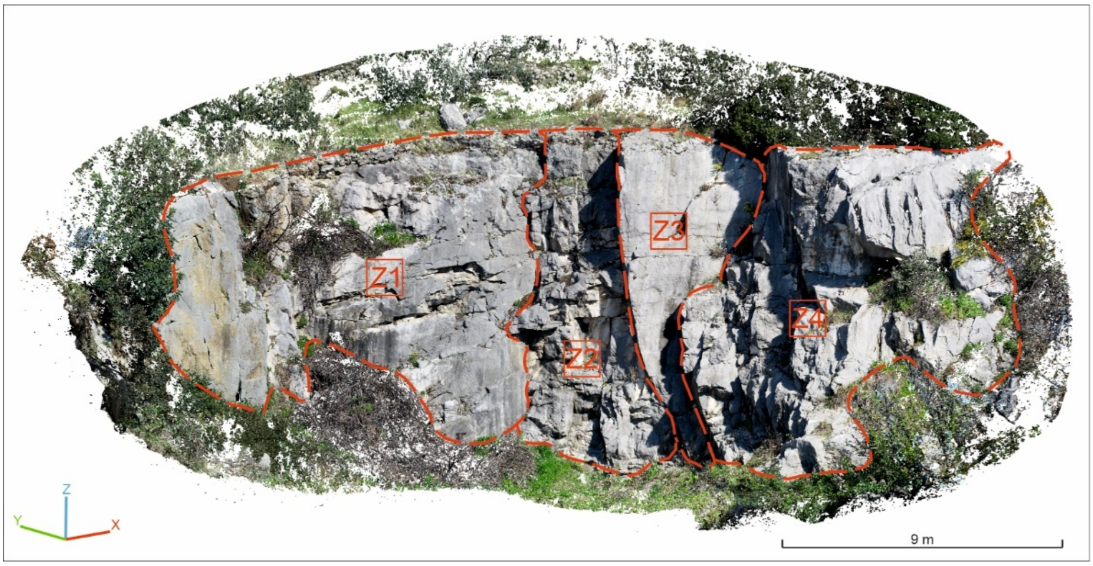

Figure 1 3D point cloud representing the rock slope with highlighted (in red) four engineering geological zones.

3D rockfall susceptibility assessment

The 3D kinematic analysis was executed to identify the potential rockfall source areas in normal dipping and overhanging slopes based on the high-resolution 3D point cloud data. Analysis was done for planar, wedge, and flexural toppling failure by applying conditions proposed by Gigli et al. (2022). The analysis made it possible to highlight points in the 3D point cloud on locations that are prone to certain types of failure. Input parameters for the 3D kinematic analysis included raw 3D point cloud data of the rock slope, orientations of the mapped discontinuity planes in the form of dip and dip direction, and average value of friction angle of 30° obtained from Vallejo and Ferrer (2011).

Based on the performed kinematic analysis for each point in the 3D point cloud, rockfall susceptibility was assessed by calculating the Kinematic Hazard Index (Casagli & Pini 1993). The KHI is calculated for each point in the 3D point cloud by calculating the percentage of discontinuity poles and discontinuity intersections that satisfy geometrical conditions for certain types of failure according to the following equations:

$$KHI_{PF} = \frac{N_{PF}}{N}\ (\%) \quad [1]$$

$$KHI_{WF} = \frac{I_{WF}}{I}\ (\%) \quad [2]$$

$$KHI_{FTF} = \frac{N_{FTF}}{N}\ (\%) \quad [3]$$

where KHI_{PF}, KHI_{WF}, and KHI_{FTF} represent calculated Kinematic Hazard Index (KHI) values for planar, wedge, and flexural toppling failures, respectively. N_{PF} and N_{FTF} denote the number of discontinuity planes meeting geometric criteria for planar and flexural toppling failures, while I_{WF} indicates the number of discontinuity intersections satisfying geometric conditions for wedge failure. N and I stand for the total number of mapped discontinuity planes and discontinuity intersections.

Results

Engineering geological mapping using 3D point cloud data resulted in the recognition of 373 individual discontinuity planes grouped into five discontinuity sets, four fracture sets (JS-1 – JS-4) and a bedding plane (JS-0) as presented in Fig. 2. Discontinuities were grouped using the Fuzzy cluster approach based on the provided discontinuity orientation data, with number of input data ranging from 24 in Z-3 up to 174 in Z-4. Based on cluster analysis, mean discontinuity set orientations were determined (Table 2).

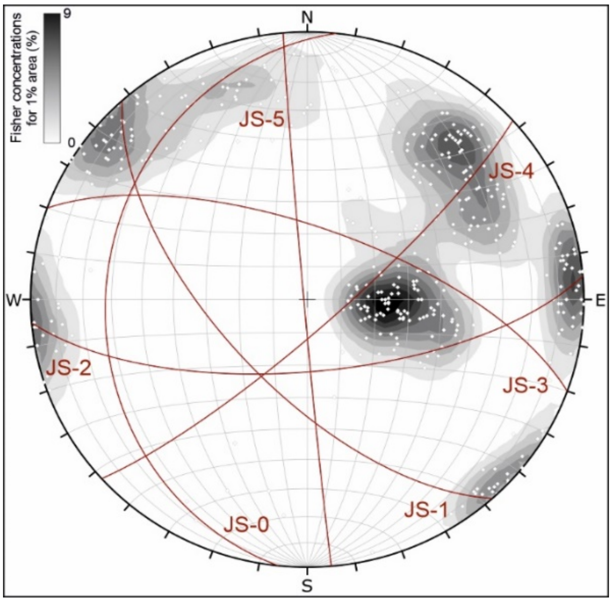

Figure 2 Stereographic projection (lower hemisphere and equal area) of the discontinuities for the study area.

Table 2 Discontinuity set orientations extracted by manual mapping in CloudCompare.

Discontinuty set ID	Slope Orientation	Zone ID
JS-0	266/29	Z1, Z2, Z3, Z4
JS-1	228/64	Z1, Z2, Z3, Z4
JS-2	170/70	Z1, Z2
JS-3	20/68	Z1
JS-4	135/82	Z2, Z3, Z4
JS-5	265/88	Z2, Z4

Results of engineering geological mapping of discontinuities were used as input data for 3D rockfall susceptibility assessment using in-house MATLAB code. Rockfall susceptibility, i.e. KHI values were assessed for planar, wedge, and flexural toppling failure. The generated rockfall susceptibility maps are presented in Fig. 3. From the maps, it is visible that the highest maximal values of KHI are observed for wedge failure (92.5%), while the lowest maximal KHI values are observed for flexural toppling failure (18%). The maximal KHI value for the planar failure mechanism is 47%.

Analysing the spatial distribution of calculated KHI values for three failure mechanisms, it is evident that flexural toppling mechanics represent an insignificant possibility of occurrence, while possible rockfalls occur due to wedge and planar failure mechanisms. Planar and wedge failure mechanisms occur at similar locations, with the most highlighted hotspot in the upper part of the engineering geological zone Z4.

Upon inspecting the 3D point cloud, it is visible that this hotspot area was previously affected by rockfall activity in its overhanging part, as shown in Fig.4. Furthermore, the majority of the potential rockfall sources are located in the overhanging areas of the rock mass.

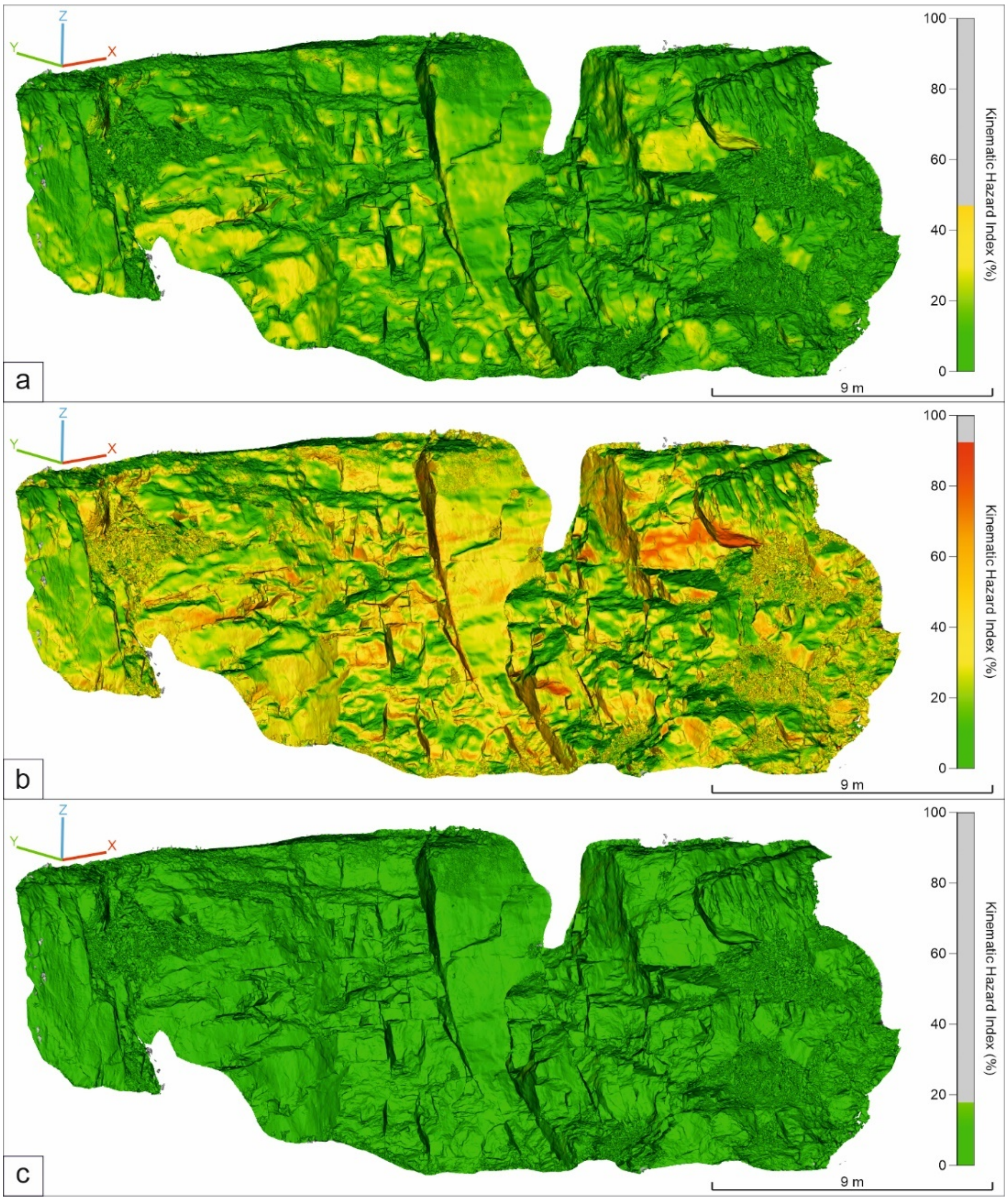

Figure 3 3D rockfall susceptibility maps produced for: a) planar failure, b) wedge failure, and c) flexural toppling failure.

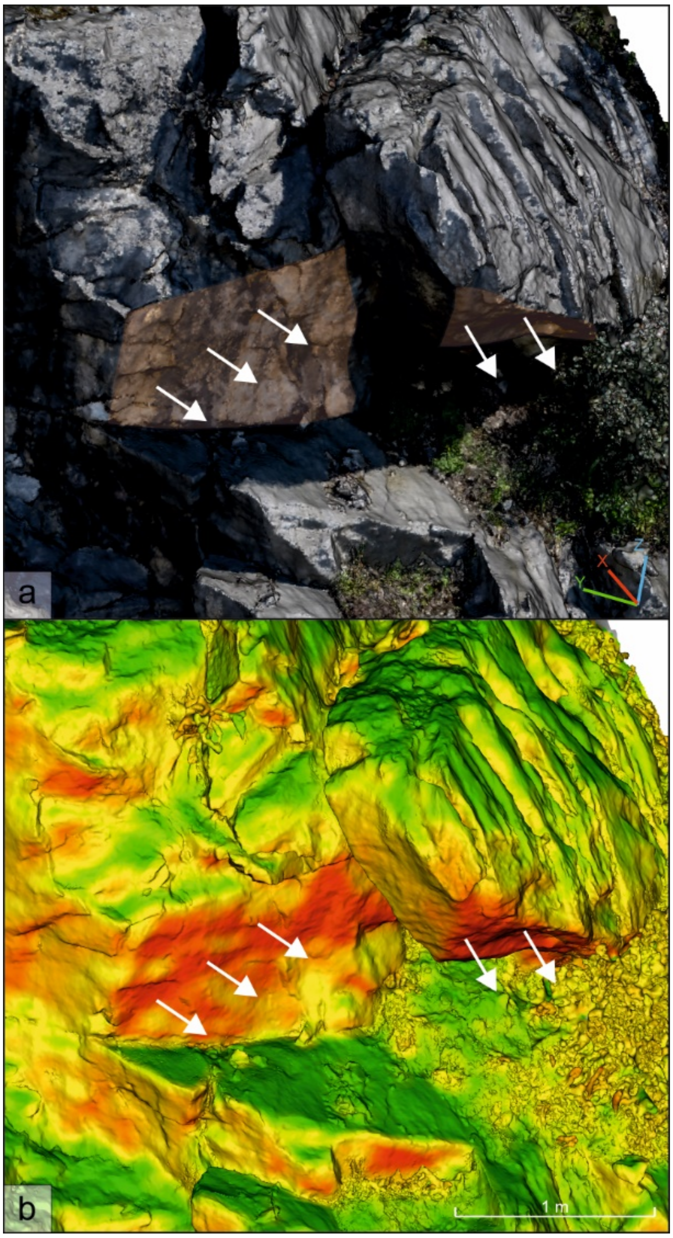

Figure 4 Close-up view on the portion of the rock slope affected by rockfall: a) Digital Outcrop Model and b) rockfall susceptibility map for wedge failure.

Discussion and conclusions

This study demonstrates the application of rapid rockfall susceptibility assessment at a detailed scale utilizing high-resolution 3D point cloud data. High-resolution 3D point cloud used for this study was obtained through UAV digital photogrammetry by applying SfM methodology.

Engineering geological mapping of discontinuity orientations, as input data from rockfall susceptibility assessment, was done on a point cloud with an average point density of 271 470 points/m^2. Mapping was performed manually using the Compass tool integrated within CloudCompare v2.12. Engineering geological mapping resulted in identifying 373 individual discontinuity planes grouped into five sets across four engineering geological zones. The acquired discontinuity orientation data were then used to conduct a comprehensive 3D rockfall susceptibility assessment by analysing three types of failure (planar, wedge, and flexural toppling).

The 3D rockfall susceptibility assessment involved spatial kinematic analysis for normal and overhanging slopes, considering complex slope topology, the data available for high-resolution 3D point cloud. The Kinematic Hazard Index (KHI) was calculated for each point of the point cloud, highlighting potential rockfall source areas. The rockfall susceptibility maps reveal that the highest KHI values are associated with a wedge failure, reaching 92.5%, whereas the lowest maximal values are associated with a flexural toppling failure, up to 18%. The planar failure mechanism exhibits maximum values of up to 47%. The spatial distribution of rockfall sources (maximal KHI values), for all types of failure, are located on the overhanging parts of the rock slope.

The results of the study indicated that the proposed approach, based on high-resolution 3D point cloud data, is useful for rapidly assessing rockfall susceptibility. The proposed approach enables insights into planar, wedge, and flexural toppling failure mechanisms, and highlights locations of the rock slope that may become unstable, providing valuable data for characterizing and mitigating rockfall hazards and for emergency measures.

References

Admassu Y, Shakoor A (2013) DIPANALYST: A computer program for quantitative kinematic analysis of rock slope failures. Comput Geosci. 54:196–202. https://doi.org/10.1016/j.cageo.2012.11.018.

Agisoft. General Image Capture Tips (2020) Available online: https://www.agisoft.com/ [Last accessed: 10 November 2023).

Battulwar R, Zare-Naghadehi M, Emami E, Sattarvand J (2021) A state-of-the-art review of automated extraction of rock mass discontinuity characteristics using three-dimensional surface models. Journal of Rock Mechanics and Geotechnical Engineering 13:920–936. https://doi.org/10.1016/j.jrmge.2021.01.008.

Brodu N, Lague D (2012) 3D terrestrial lidar data classification of complex natural scenes using a multi-scale dimensionality criterion: Applications in geomorphology. ISPRS Journal of Photogrammetry and Remote Sensing 68:121–134. https://doi.org/10.1016/j.isprsjprs.2012.01.006.

Casagli N, Pini N (1993) Analisi cinematica della stabilità di versanti naturali e fronti di scavo in roccia. Geol Appl Idrogeo 28:223–232.

Evans SG, Hungr O (1993) The assessment of rockfall hazard at the base of talus slopes. Canadian Geotechnical Journal 30:620–636. https://doi.org/10.1139/t93-054.

Fanti R, Gigli G, Lombardi L, Tapete D, Canuti P (2013) Terrestrial laser scanning for rockfall stability analysis in the cultural heritage site of Pitigliano (Italy). Landslides 10:409–420. https://doi.org/10.1007/s10346-012-0329-5

Farmakis I, Hutchinson DJ, Vlachopoulos N, Westoby M, Lim M (2023) Slope-Scale rockfall susceptibility modeling as a 3D computer

vision problem. Remote Sens (Basel) 15:2712. https://doi.org/10.3390/rs15112712
Farmakis I, Marinos V, Papathanassiou G, Karantanellis E (2020) Automated 3D jointed rock mass structural analysis and characterization using LiDAR terrestrial laser scanner for rockfall susceptibility assessment: Perissa Area Case (Santorini). Geotechnical and Geological Engineering 38:3007–3024. https://doi.org/10.1007/s10706-020-01203-x
Geological survey Sarajevo Sarajevo (1967) Basic Geological Map, scale 1:100 000, Trebinje sheet.
Gigli G, Frodella W, Mugnai F, Tapete D, Cigna F, Fanti R, Intrieri E, Lombardi L (2012) Instability mechanisms affecting cultural heritage sites in the Maltese Archipelago. Natural Hazards and Earth System Sciences 12:1883–1903. https://doi.org/10.5194/nhess-12-1883-2012.
Gigli G, Lombardi L, Carlà T, Beni T, Casagli N (2022) A method for full three-dimensional kinematic analysis of steep rock walls based on high-resolution point cloud data. International Journal of Rock Mechanics and Mining Sciences 157:105178. https://doi.org/10.1016/j.ijrmms.2022.105178.
Gonzalez de Vallejo L, Ferrer M (2011) Geological Engineering. CRC Press. 700p.
Loye A, Jaboyedoff M, Pedrazzini A (2009) Identification of potential rockfall source areas at a regional scale using a DEM-based geomorphometric analysis. Natural Hazards and Earth System Sciences 9:1643–1653. https://doi.org/10.5194/nhess-9-1643-2009.
Luhmann T, Robson S, Kyle S, Boehm J (2019) Closer-range photogrammetry and 3D imaging. De Gruyter.
Matasci B, Stock GM, Jaboyedoff M, Carrea D, Collins BD, Guérin A, Matasci G, Ravanel L (2017) Assessing rockfall susceptibility in steep and overhanging slopes using three-dimensional analysis of failure mechanisms. Landslides 15:859–878. https://doi.org/10.1007/s10346-017-0911-y.
Mauro Rossi Paola Reichenbach Rosa María Mateos RS (2021) Probabilistic identification of rockfall source areas at regional scale in El Hierro (Canary Islands, Spain). Geomorphology 281.
MathWorks Inc (2023) Available online: https://www.mathworks.com [Last accessed: 8 October 2023).
Menegoni N, Giordan D, Perotti C (2021) An open-source algorithm for 3D rock slope kinematic analysis (ROKA). Applied Sciences 11:1698. https://doi.org/10.3390/app11041698.
Rocscience (2022) Available online: https://www.rocscience.com/software/dips [Last accessed: 3 November 2023).
Thiele ST, Grose L, Samsu A, Micklethwaite S, Vollgger SA, Cruden AR (2017) Rapid, semi-automatic fracture and contact mapping for point clouds, images and geophysical data. Solid Earth 8:1241–1253. https://doi.org/10.5194/se-8-1241-2017.
Wehr A, Lohr U (1999) Airborne laser scanning—an introduction and overview. ISPRS Journal of Photogrammetry and Remote Sensing 54:68–82. https://doi.org/10.1016/S0924-2716(99)00011-8